International Journal of Applied Pharmaceutics

ISSN- 0975-7058 Vol 16, Issue 1, 2024

Original Article

VIRTUAL SCREENING OF FDA-APPROVED DRUGS BY MOLECULAR DOCKING AND DYNAMICS SIMULATION TO RECOGNIZE POTENTIAL INHIBITORS AGAINST *MYCOBACTERIUM TUBERCULOSIS* ENOYL-ACYL CARRIER PROTEIN REDUCTASE ENZYME

HASANAIN ABDULHAMEED ODHAR*, AHMED FADHIL HASHIM, SALAM WAHEED AHJEL, SUHAD SAMI HUMADI

Department of pharmacy, Al-Zahrawi University College, Karbala, Iraq
***Corresponding author: Hasanain Abdulhameed Odhar; *Email: hodhar3@gmail.com**

Received: 23 Sep 2023, Revised and Accepted: 28 Oct 2023

ABSTRACT

Objective: This *in silico* study is aimed at identification of new possible inhibitors against *Mycobacterium tuberculosis* InhA enzyme by screening a library of FDA-approved drugs.

Methods: In this *in silico* study, a library of FDA-approved drugs was screened by molecular docking against the monomer of enoyl-acyl carrier protein reductase to recognize potential inhibitors. Then, those best drugs with minimum docking energy were subjected to molecular dynamics simulation.

Results: Out of the top ten docking hits, only revefenacin was able to maintain the closet proximity to InhA enzyme binding pocket during the two rounds of dynamics simulation. Analysis of molecular dynamics (MD) simulation data indicated that the antimuscarinic drug revefenacin has a ligand movement Root-Mean-Square Deviation (RMSD) that didn't exceed 4 Angstrom. Also, in this MD study, revefenacin has a superior binding energy of -35.59 Kcal/mol as compared to -13.88 Kcal/mol for the other hit ergotamine. These favorable MD simulation records for revefenacin can be explained by its ability to continuously interact with enzyme binding pocket by two hydrogen bonds.

Conclusion: We report that the antimuscarinic drug revefenacin may have the potential to inhibit the enoyl-acyl carrier protein reductase for *Mycobacterium tuberculosis*. However, these preliminary results must be further evaluated by *in vitro* and *in vivo* studies.

Keywords: Docking, Dynamics simulation, Repurpose, *Mycobacterium tuberculosis*, Enoyl-acyl carrier protein reductase, InhA

DOI: https://dx.doi.org/10.22159/ijap.2024v16i1.49471 Journal homepage: https://innovareacademics.in/journals/index.php/ijap

INTRODUCTION

Tuberculosis (TB) is one of the earliest recognized infective diseases in human history that is caused by the aerobic bacillus bacterium called *Mycobacterium tuberculosis* [1]. This acid-fast pathogen can be transmitted by the inhalation of respiratory droplets that usually generated by the coughing of active TB patients [2]. Once the bacilli of *Mycobacterium tuberculosis* reach the respiratory alveoli, it will then get phagocytized by the resident alveolar macrophages. Some of these engulfed bacilli will continue to multiply inside macrophages, leading to the lysis of these innate immune cells. If the alveolar macrophages failed to eliminate *Mycobacterium tuberculosis* infection within one to two weeks, then local inflammation will recruit monocytes to the site of infection with subsequent establishment of specific T-cells mediated immune response. When immune cells are unable to eradicate infection by *Mycobacterium tuberculosis*, then the best strategy to prevent further spread of infection is by the formation of granuloma around mycobacterial bacilli [3]. It is estimated that in about 10% of *Mycobacterium tuberculosis* infection cases, immune cells will succuss to eliminate infection. However, in most infection cases, some mycobacterial bacilli will escape immune response and enter a latent and non-replicating stage in lesion areas of the lung, leading to a latent tuberculosis infection (LTBI). These dormant bacilli can regain their ability to multiply and spread when immune system is disrupted, leading to active tuberculosis infection [4]. According to the estimates of World Health Organization (WHO), about one-quarter of world population is latently infected with *Mycobacterium tuberculosis* and 5-10 % of them will later develop active TB (https://www.who.int/news-room/fact-sheets/detail/tuberculosis) [5, 6]. In active TB cases, the immune cells will fail to contain mycobacterial infection and bacilli can spread through blood circulation and lymphatic channels into other distal parts of the body. This can result in a serious damage in lung and other parts of the body like the brain, spinal cord and bones. Usually, individuals with latent TB are asymptomatic and can't transmit infection. On the contrary, actively infected patients can spread the infection to others and experience clinical symptoms like continuous coughing, bloody sputum, fatigue, fever and chest pain [7]. For the effective management of TB cases, rapid and reliable diagnostic methods must be utilized. The frequently used methods for diagnosis of TB cases are clinical diagnosis, chest X-ray, microscopic identification, bacterial culture and immunologic tests like skin test [8]. Also, early and effective treatment is important in the management of TB to avoid the emergence of drug-resistant strains of *Mycobacterium tuberculosis*. The standard treatment regimen recommended by WHO for active pulmonary TB involves the administration of four antibiotics in combination for two months and these are: isoniazid (INH), rifampicin, ethambutol and pyrazinamide. After that, a combination of only isoniazid and rifampicin is used for another four months [9]. Unfortunately, this long and complex TB treatment regimen has led to issues like patient non-compliance with subsequent treatment failure [10]. The failure of treatment can lead to TB relapse and emergence of either multidrug-resistant tuberculosis (MDR-TB) or extensively drug-resistant tuberculosis (XDR-TB) [11]. Moreover, the only available tuberculosis vaccine is the Bacillus of Calmette and Guérin (BCG) vaccine, whose efficacy is controversial and can range between 0-80 % according to clinical trials [12]. Therefore, it is relevant to introduce new therapeutic agents that can reduce the current burden of public health threat imposed by TB. In this direction, one of the potential molecular targets to design new anti-tuberculosis agents is the mycolic acids (MAs) synthesis pathway. The mycolic acids are long chain fatty acids that are essential for the buildup and integrity of mycobacterium cell wall. These fatty acids can act as a permeability barrier and contribute to bacterial resistance against both host defense mechanisms and different antibiotics [13, 14]. In *Mycobacterium tuberculosis*, one of the key enzymes for the reduction stage of fatty acids production and biosynthesis of mycolic acids is the enoyl-acyl carrier protein (ACP) reductase (InhA). The InhA is an NADH-dependent reductase and is a well-known target for isoniazid (INH) [15]. As such, we have chosen in this *in silico* study the enoyl-ACP reductase of *Mycobacterium tuberculosis* as a molecular target to screen a library of FDA-approved drugs. This

virtual screening study is aimed at the identification of new potential inhibitors against *Mycobacterium tuberculosis* InhA enzyme.

MATERIALS AND METHODS

Setting up a virtual screening study plan

The main steps and options applied in this *in silico* study are outlined in (fig. 1). As noted in this figure, both molecular docking and two rounds of dynamics simulation were employed to virtually screen a library of FDA approved drugs against *Mycobacterium tuberculosis* InhA enzyme.

Molecular docking

For this computational study, we have used the online drug discovery web server named DrugRep to virtually screen a library of 2,315 FDA-approved drugs against chain A of enoyl-ACP reductase for *Mycobacterium tuberculosis* [16]. Initially, chain A only of the enoyl-ACP reductase (PDB: 1BVR) was extracted by using UCSF Chimera version 1.15 [17, 18]. Then, this extracted monomer of InhA enzyme was uploaded to the DrugRep server to perform a structure-based virtual screening. It is worthwhile to mention that the DrugRep website utilizes both AutoDockTools version 1.5.6 and AutoDock Vina version 1.1.2 to prepare the uploaded target and perform the docking step, respectively [19, 20]. In this study, the used docking coordinates were X: 17.0, Y: 14.0, Z: 8.0 while the dimensions of grid box were 22*22*22 Angstrom. Moreover, the accuracy of this docking protocol was assessed by redocking the co-crystalized NAD^+into chain A of enoyl-ACP reductase. Then, PacDOCK web server was used to compare the conformation of co-crystalized and docked $NAD^+$by calculating the root mean square deviation (RMSD) [21]. Finally, we have selected the best 10 drugs with least docking energy for more assessment by molecular dynamics (MD) simulation. Additionally, the orientation of least binding energy pose for each drug-enzyme docking complex was visualized by using PyMOL version 2.4.1 (https://pymol.org/2/) and protein-ligand interaction profiler (PLIP) [22]. It should be noted that during selecting the top 10 hits, we have removed anticancer, antihypertensive and psychoactive drugs from the results of this virtual screening as the use of these agents can be associated with unacceptable adverse effects. Thus, the repurpose of these drugs may be clinically inappropriate for tuberculosis patients.

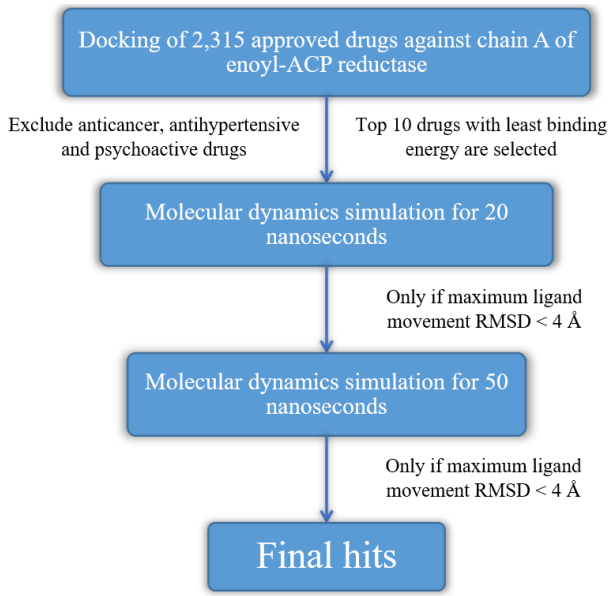

Fig. 1: An outline for the main steps and options of the applied virtual screening study

Molecular dynamics (MD) simulation study

After molecular docking, YASARA Dynamics version 20.12.24 was utilized to carry out two rounds of molecular dynamics simulation for 20 and 50 nanoseconds intervals [23]. In the first round of MD simulation, the drug-enzyme docking complex with least energy binding pose for each of the top 10 hits was submitted to undergo 20 nanoseconds simulation. After that, only those drugs with maximum proximity RMSD to enoyl-ACP reductase binding pocket of less than 4 Angstrom were submitted to the second round of 50 nanoseconds simulation. Again, the ligand maximum proximity RMSD to the enzyme active site was calculated to validate results of MD simulation second round. In addition, the binding energy of molecular mechanics Poisson-Boltzmann surface area (MM-PBSA) was computed for each drug by using AMBER14 force field [24]. For this MD study, the detailed procedure and applied options are identical to what we have used in our previously published studies [25–27]. Concisely, NaCl was employed in this simulation with a concentration of 0.9%. Also, an excess concentration of either Na^+ or Cl^- ions was applied to the simulation environment to ensure the neutralization of the drug-enzyme complex. This MD simulation was carried out with the help of the following force fields: AM1BCC and GAFF2 for the ligand, AMBER14 for the solute, TIP3P for water [24, 28, 29]. Moreover, any probability of clashes in this simulation was prohibited through the reduction of the steepest descent and simulated annealing.

RESULTS AND DISCUSSION

Before starting the virtual screening study, the precision of the followed docking protocol was assessed first by using the redocking method. In this method, the co-crystalized NAD^+ was removed from chain A of InhA enzyme and docked again into the same binding pocket by using similar procedure and options to those applied in the virtual screening project. Then, the native conformation of NAD^+ was aligned with the docked conformation and RMSD value was calculated to estimate the variation degree between these two conformations. It is well-known that a lower RMSD value for conformations variation reflects good accuracy of docking protocol. According to literatures review, a precise docking protocol is usually coincided with a conformations difference RMSD between 1.5 and 2.0 Angstrom [30]. In this study, the alignment of NAD^+ native conformation with the docked one can be observed in (fig. 2). As seen in this figure, the computed RMSD value for conformations difference was 1.58 Angstrom. Thus, the applied docking protocol for this study is deemed to be accurate. It should be pointed out that the docking energy of NAD^+ into chain A of enoyl-ACP reductase was -9.4 Kcal/mol.

An overview for the results of molecular docking and dynamics simulation study for the best 10 drugs can be observed in (table 1). Based on findings in this table, the docking energy for these drugs is ranging between -12.1 and-9.6 Kcal/mol. interestingly, the first three

hits in (table 1) with least binding energy are anti-migraine medications. Also, two of the hits listed in (table 1) are penicillin antibiotics and these are carindacillin and sultamicillin. According to several published studies, many of the listed drugs in (table 1) may have activity against viruses like SARS-CoV-2 and West Nile virus [31–36]. Moreover, based on an *in vitro* study, the anti-asthma drug zafirlukast may have antituberculosis activity. In this study, zafirlukast was able to inhibit the growth of *Mycobacterium tuberculosis* by causing a dysregulation in the expression of several genes inside bacteria [37]. However, the maximum ligand movement RMSD in the first round of MD simulation in (table 1) indicated that only ergotamine and revefenacin were able to stay close to binding site with RMSD value less than 4 Angstrom throughout 20 nanoseconds interval. It is well-known that a low ligand movement RMSD means a close proximity of the drug to target site and, thus stronger binding [38]. Consequently, the second round of MD simulation for 50 nanoseconds were executed only for ergotamine and revefenacin. During this later simulation, only the antimuscarinic drug revefenacin was able to maintain a ligand movement RMSD value that didn't exceed 4 Angstrom as seen in the last column in (table 1).

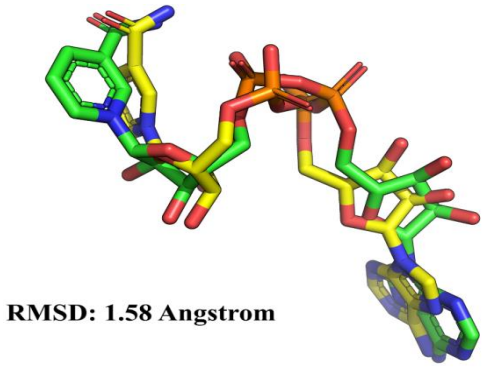

Fig. 2: An alignment of NAD^+ native conformation (green color) with the docked conformation (yellow color)

Table 1: A tabular summary of the molecular docking and dynamics simulation (MD) study results for the top 10 FDA-approved drugs that were virtually screened against the monomer of *Mycobacterium tuberculosis* enoyl-acyl carrier protein reductase (InhA). These top hits were listed based on their least docking energy of binding to chain A of InhA enzyme

No.	Generic name	Clinical indications	Docking energy (Kcal/mol)	Maximum ligand movement RMSD (Å)	
				20 nanoseconds	50 nanoseconds
1	Ergotamine	Migraine	-12.1	3.92	4.20
2	Rimegepant	Migraine	-12.0	6.65	-
3	Ubrogepant	Migraine	-11.5	6.26	-
4	Conivaptan	Hyponatremia	-11.4	4.21	-
5	Zafirlukast	Asthma	-10.1	5.99	-
6	Revefenacin	Chronic obstructive pulmonary disease	-10.1	3.40	3.40
7	Ebastine	Allergy	-10.0	7.87	-
8	Carindacillin	Bacterial infection	-9.9	6.93	-
9	Sultamicillin	Bacterial infection	-9.7	6.78	-
10	Glimepiride	Type 2 diabetes mellitus	-9.6	7.12	-

RMSD: Root-Mean-Square Deviation; Å: Angstrom.

A detailed plot of ligand movement RMSD throughout 50 nanoseconds interval of MD simulation can be viewed in (fig. 3) for both ergotamine and revefenacin. Based on this plot, it is expected that revefenacin was able to stay closer than ergotamine to the binding site of InhA enzyme monomer. As a result, revefenacin may exhibit a stronger binding potential to enzyme active site because it has a lower ligand movement RMSD values during MD simulation. Moreover, the computed average MM-PBSA binding energy during 50 nanoseconds simulation was -13.88 and-35.59 Kcal/mol for ergotamine and revefenacin, respectively.

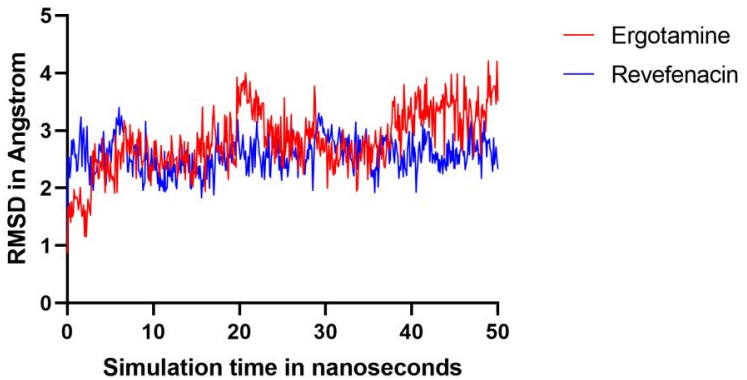

Fig. 3: A plot of ligand movement RMSD versus molecular dynamics simulation interval for both ergotamine and reverencing

This difference in ligand movement RMSD and MM-PBSA binding energy during MD simulation between ergotamine and revefenacin can be explained through examination of types of interactions between drug and residues of enzyme binding pocket. The visualization of docking complexes in (fig. 4), indicated that both ergotamine and revefenacin can form two hydrogen bonds with residues of enzyme binding site. However, only revefenacin was able to keep these two hydrogen bonds with enzyme active site throughout 50 nanoseconds of MD simulation as can be noted in (fig. 5). Hence, during MD simulation, the closer proximity and favorable binding energy for revefenacin can be explained by the ability of this antimuscarinic agent to maintain these two hydrogen bonds with InhA enzyme.

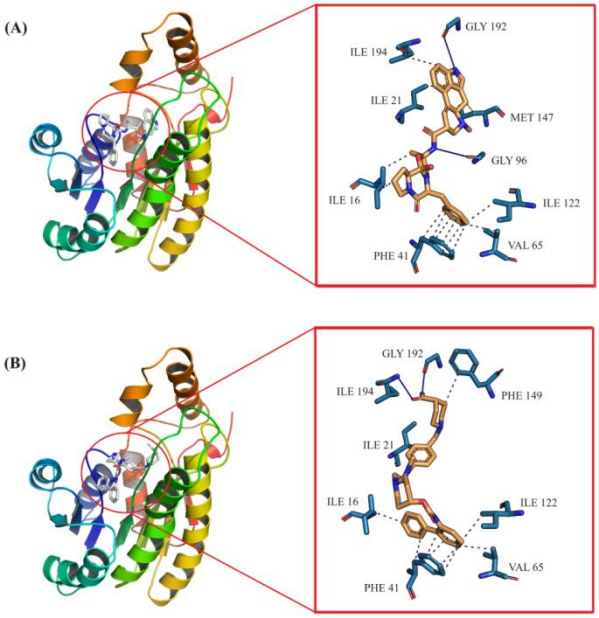

Fig. 4: A graphical illustration of docking complex for (A) ergotamine and (B) revefenacin. Hydrogen bond is illustrated as blue continuous line while hydrophobic bond is represented by the dashed line

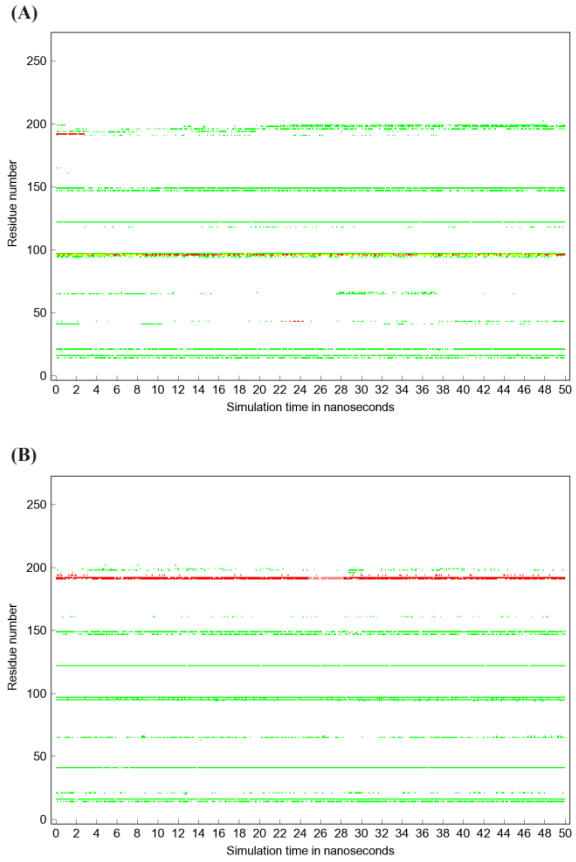

Fig. 5: A plot for types of ligand-enzyme interactions as a function of simulation interval for (A) ergotamine and (B) revefenacin. Hydrogen bonds are represented by red color and hydrophobic interaction is illustrated by green color

CONCLUSION

In this computational study, we report that the bronchodilator drug revefenacin may have the capacity to inhibit enoyl-ACP reductase (InhA) enzyme for *Mycobacterium tuberculosis*. Both molecular docking and dynamics simulation analysis pointed to the possible ability of revefenacin to maintain hydrogen bonds interaction with enzyme binding pocket during simulation. This continuous interaction ability may explain the closer proximity of revefenacin to InhA binding pocket and its favorable binding energy as compared to other virtual screening hits. However, these preliminary results must be further validated by *in vitro* and *in vivo* studies.

FUNDING

Nil

AUTHORS CONTRIBUTIONS

All authors have contributed equally.

CONFLICT OF INTERESTS

The authors declare no conflict of interests.

REFERENCES

1. Gordon SV, Parish T. Microbe profile: mycobacterium tuberculosis: humanity's deadly microbial foe. Microbiology (Reading). 2018 Apr 1;164(4):437-9. doi: 10.1099/MIC.0.000601, PMID 29465344.
2. Churchyard G, Kim P, Shah NS, Rustomjee R, Gandhi N, Mathema B. What we know about tuberculosis transmission: an overview. J Infect Dis. 2017;216 Suppl 6:S629-35. doi: 10.1093/INFDIS/JIX362, PMID 29112747.
3. Eruslanov EB, Majorov KB, Orlova MO, Mischenko VV, Kondratieva TK, Apt AS. Lung cell responses to M. tuberculosis in genetically susceptible and resistant mice following intratracheal challenge. Clin Exp Immunol. 2004 Jan;135(1):19-28. doi: 10.1111/j.1365-2249.2004.02328.x, PMID 14678260.
4. Ahmad S. Pathogenesis, immunology, and diagnosis of latent mycobacterium tuberculosis infection. Clin Dev Immunol. 2011;2011:814943. doi: 10.1155/2011/814943, PMID 21234341.
5. Dasan N, Babu G, George S. Molecular docking studies and synthesis of 3, 4 – disubstituted triazoles as mycobacterium tuberculosis enoyl-acp reductase and cyp-51 inhibitors. Int J Pharm Pharm Sci. 2019 Jan 1;11(1):85-91. doi: 10.22159/IJPPS.2019V11I1.29428.
6. Asnawi A, Febrina E, Aligita W, Kurnia D, Aman LO, Yuliantini A. Screening of ASHITABA (angelica KEISKEI K.) compounds as potential mycobacterium tuberculosis KASA inhibitors. Int J App Pharm. 2022 Dec 27;14Special Issue 5:80-5. doi: 10.22159/ijap.2022.v14s5.13.
7. Munoz L, Stagg HR, Abubakar I. Diagnosis and management of latent tuberculosis infection. Cold Spring Harb Perspect Med. 2015 Nov 1;5(11):A017830. doi: 10.1101/cshperspect.a017830, PMID 26054858.
8. Acharya B, Acharya A, Gautam S, Ghimire SP, Mishra G, Parajuli N. Advances in diagnosis of tuberculosis: an update into the molecular diagnosis of mycobacterium tuberculosis. Mol Biol Rep. 2020 May 1;47(5):4065-75. doi: 10.1007/S11033-020-05413-7, PMID 32248381.
9. Chideya S, Winston CA, Peloquin CA, Bradford WZ, Hopewell PC, Wells CD. Isoniazid, rifampin, ethambutol, and pyrazinamide pharmacokinetics and treatment outcomes among a predominantly HIV-infected cohort of adults with tuberculosis from botswana. Clin Infect Dis. 2009 Jun 6;48(12):1685-94. doi: 10.1086/599040, PMID 19432554.
10. Shaji J, Shaikh M. Drug-resistant tuberculosis: recent approach in polymer-based nanomedicine. Int J Pharm Pharm Sci. 2016 Oct 1;8(10):1-6. doi: 10.22159/IJPPS.2016V8I10.11295.
11. Seung KJ, Keshavjee S, Rich ML. Multidrug-resistant tuberculosis and extensively drug-resistant tuberculosis. Cold Spring Harb Perspect Med. 2015;5(9):a017863. doi: 10.1101/cshperspect.a017863, PMID 25918181.
12. Cho T, Khatchadourian C, Nguyen H, Dara Y, Jung S, Venketaraman V. A review of the BCG vaccine and other approaches toward tuberculosis eradication. Hum Vaccin Immunother. 2021 Aug;17(8):2454-70. doi: 10.1080/21645515.2021.1885280, PMID 33769193.
13. Jarlier V, Nikaido H. Mycobacterial cell wall: structure and role in natural resistance to antibiotics. FEMS Microbiol Lett. 1994 Oct;123(1-2):11-8. doi: 10.1111/j.1574-6968.1994.tb07194.x, PMID 7988876.
14. Kremer LS, Besra GS. Current status and future development of antitubercular chemotherapy. Expert Opin Investig Drugs. 2002 Aug;11(8):1033-49. doi: 10.1517/13543784.11.8.1033, PMID 12150700.
15. Rotta M, Pissinate K, Villela AD, Back DF, Timmers LFSM, Bachega JFR. Piperazine derivatives: synthesis, inhibition of the mycobacterium tuberculosis enoyl-acyl carrier protein reductase and SAR studies. Eur J Med Chem. 2015 Jan;90:436-47. doi: 10.1016/j.ejmech.2014.11.034, PMID 25461892.
16. Gan JH, Liu JX, Liu Y, Chen SW, Dai WT, Xiao ZX. DrugRep: an automatic virtual screening server for drug repurposing. Acta Pharmacol Sin. 2023 Apr;44(4):888-96. doi: 10.1038/s41401-022-00996-2, PMID 36216900.
17. Rozwarski DA, Vilchèze C, Sugantino M, Bittman R, Sacchettini JC. Crystal structure of the mycobacterium tuberculosis enoyl-ACP reductase, InhA, in complex with NAD^+ and a C16 fatty acyl substrate. J Biol Chem. 1999 May;274(22):15582-9. doi: 10.1074/jbc.274.22.15582, PMID 10336454.
18. Pettersen EF, Goddard TD, Huang CC, Couch GS, Greenblatt DM, Meng EC. UCSF Chimera-a visualization system for exploratory research and analysis. J Comput Chem. 2004 Oct;25(13):1605-12. doi: 10.1002/JCC.20084, PMID 15264254.
19. Morris GM, Huey R, Lindstrom W, Sanner MF, Belew RK, Goodsell DS. AutoDock4 and AutoDockTools4: automated docking with selective receptor flexibility. J Comput Chem. 2009 Dec;30(16):2785-91. doi: 10.1002/JCC.21256, PMID 19399780.
20. Trott O, Olson AJ. AutoDock vina: improving the speed and accuracy of docking with a new scoring function, efficient optimization, and multithreading. J Comput Chem. 2010 Jan 1;31(2):455-61. doi: 10.1002/JCC.21334, PMID 19499576.
21. Carbone J, Ghidini A, Romano A, Gentilucci L, Musiani F. PacDOCK: a web server for positional distance-based and interaction-based analysis of docking results. Molecules. 2022 Oct 1;27(20). doi: 10.3390/molecules27206884, PMID 36296477.
22. Salentin S, Schreiber S, Haupt VJ, Adasme MF, Schroeder M. PLIP: fully automated protein-ligand interaction profiler. Nucleic Acids Res. 2015;43(W1):W443-7. doi: 10.1093/NAR/GKV315, PMID 25873628.
23. Krieger E, Vriend G. Yasara view–molecular graphics for all devices–from smartphones to workstations. Bioinformatics. 2014 Oct 15;30(20):2981-2. doi: 10.1093/BIOINFORMATICS/BTU426, PMID 24996895.
24. Wang J, Wolf RM, Caldwell JW, Kollman PA, Case DA. Development and testing of a general amber force field. J Comput Chem. 2004 Jul 15;25(9):1157-74. doi: 10.1002/JCC.20035, PMID 15116359.
25. Abdulhameed Odhar H, Fadhil Hashim A, Sami Humad S. Molecular docking analysis and dynamics simulation of salbutamol with the monoamine oxidase B (MAO-B) enzyme. Bioinformation. 2022;18(3):304-9. doi: 10.6026/97320630018304, PMID 36518132.
26. Hashim AF, Odhar HA, Ahjel SW. Molecular docking and dynamics simulation analysis of nucleoprotein from the crimea-congo hemorrhagic fever virus strain baghdad-12 with FDA-approved drugs. Bioinformation. 2022;18(5):442-9. doi: 10.6026/97320630018442, PMID 36945218.
27. Odhar HA, Hashim AF, Ahjel SW, Humadi SS. Molecular docking and dynamics simulation analysis of the human FXIIa with compounds from the mcule database. Bioinformation. 2023;19(2):160-6. doi: 10.6026/97320630019160, PMID 37814681.
28. Jakalian A, Jack DB, Bayly CI. Fast, efficient generation of high-quality atomic charges. AM1-BCC model: II. Parameterization and validation. J Comput Chem. 2002 Dec;23(16):1623-41. doi: 10.1002/JCC.10128, PMID 12395429.
29. Maier JA, Martinez C, Kasavajhala K, Wickstrom L, Hauser KE, Simmerling C. ff14SB: improving the accuracy of protein side chain and backbone parameters from ff99SB. J Chem Theory

Comput. 2015 Jul 7;11(8):3696-713. doi: 10.1021/acs.jctc.5b00255, PMID 26574453.

30. Hevener KE, Zhao W, Ball DM, Babaoglu K, Qi J, White SW. Validation of molecular docking programs for virtual screening against dihydropteroate synthase. J Chem Inf Model. 2009 Feb 23;49(2):444-60. doi: 10.1021/CI800293N, PMID 19434845.
31. Gurung AB, Ali MA, Lee J, Abul Farah M, Al-Anazi KM. *In silico* screening of FDA approved drugs reveals ergotamine and dihydroergotamine as potential coronavirus main protease enzyme inhibitors. Saudi J Biol Sci. 2020 Oct 1;27(10):2674-82. doi: 10.1016/j.sjbs.2020.06.005, PMID 32837219.
32. Gul S, Ozcan O, Asar S, Okyar A, Barıs I, Kavakli IH. *In silico* identification of widely used and well-tolerated drugs as potential SARS-CoV-2 3C-like protease and viral RNA-dependent RNA polymerase inhibitors for direct use in clinical trials. J Biomol Struct Dyn. 2021;39(17):6772-91. doi: 10.1080/07391102.2020.1802346, PMID 32752938.
33. Pooventhiran T, Marondedze EF, Govender PP, Bhattacharyya U, Rao DJ, Aazam ES. Energy and reactivity profile and proton affinity analysis of rimegepant with special reference to its potential activity against SARS-CoV-2 virus proteins using molecular dynamics. J Mol Model. 2021 Oct 1;27(10):276. doi: 10.1007/S00894-021-04885-Z, PMID 34480634.
34. Mehyar N, Mashhour A, Islam I, Alhadrami HA, Tolah AM, Alghanem B. Discovery of zafirlukast as a novel SARS-CoV-2 helicase inhibitor using *in silico* modelling and a FRET-based assay. SAR QSAR Environ Res. 2021;32(12):963-83. doi: 10.1080/1062936X.2021.1993995, PMID 34818959.
35. Martinez AA, Espinosa BA, Adamek RN, Thomas BA, Chau J, Gonzalez E. Breathing new life into West Nile virus therapeutics; discovery and study of zafirlukast as an NS2B-NS3 protease inhibitor. Eur J Med Chem. 2018 Sep 5;157:1202-13. doi: 10.1016/j.ejmech.2018.08.077, PMID 30193218.
36. Charoute H, Elkarhat Z, Elkhattabi L, El Fahime E, Oukkache N, Rouba H. Computational screening of potential drugs against COVID-19 disease: the neuropilin-1 receptor as a molecular target. Virus Disease. 2022 Mar 1;33(1):23-31. doi: 10.1007/S13337-021-00751-X, PMID 35079600.
37. Pinault L, Han JS, Kang CM, Franco J, Ronning DR. Zafirlukast inhibits complexation of Lsr2 with DNA and growth of mycobacterium tuberculosis. Antimicrob Agents Chemother. 2013 May;57(5):2134-40. doi: 10.1128/AAC.02407-12, PMID 23439641.
38. Odhar HA, Ahjel SW, Albeer AAMA, Hashim AF, Rayshan AM, Humadi SS. Molecular docking and dynamics simulation of FDA-approved drugs with the main protease from 2019 novel coronavirus. Bioinformation. 2020 Mar 31;16(3):236-44. doi: 10.6026/97320630016236, PMID 32308266.